List of figures:

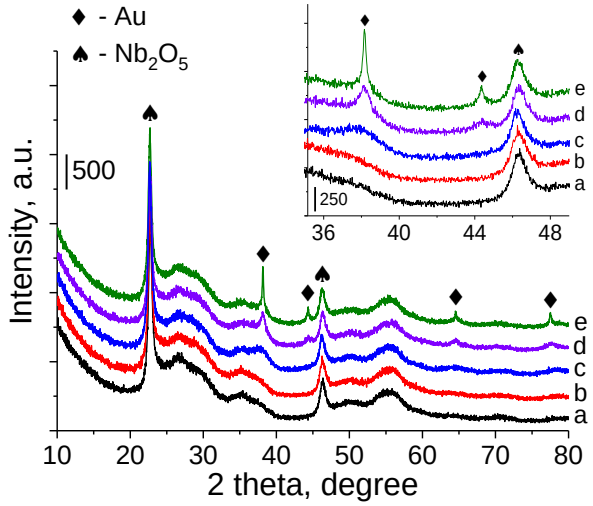

Fig. 1. XRD patterns of (a) Nb_2O_5, (b) Cu-Nb_2O_5, (c) Au-Nb_2O_5 AP, (d) AuCu-Nb_2O_5 DR and (e) Au-Nb_2O_5 DR.

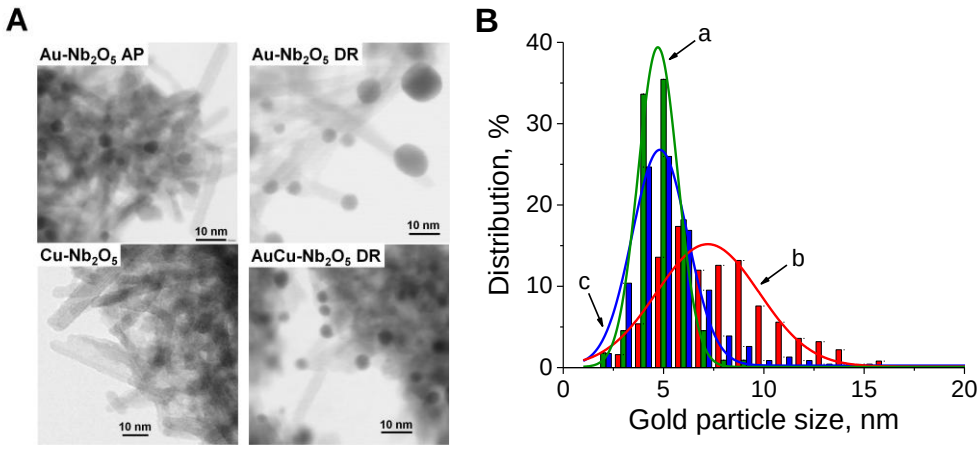

Fig. 2. (A) Representative TEM images of the catalysts and **(B)** gold particle size distribution in (a) Au-Nb_2O_5 AP, (b) Au-Nb_2O_5 DR and (c) AuCu-Nb_2O_5 DR samples basing on the TEM images.

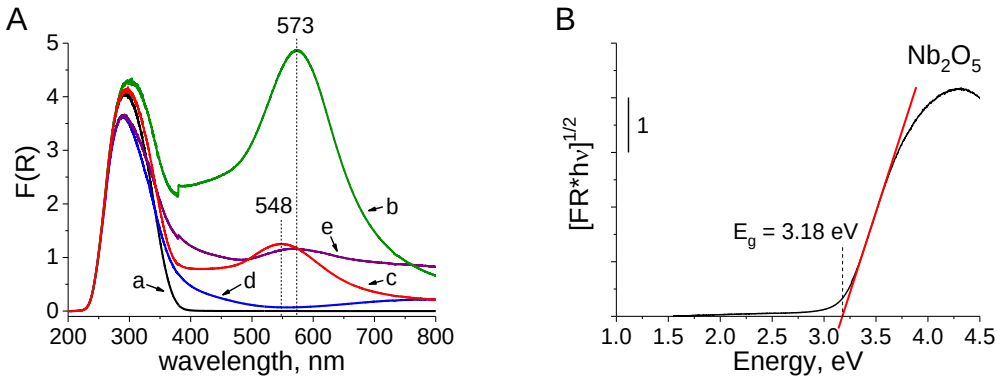

Fig. 3. (A) UV-vis spectra of (a) Nb_2O_5, (b) Au-Nb_2O_5 AP, (c) Au-Nb_2O_5 DR, (d) Cu-Nb_2O_5 and (e) AuCu-Nb_2O_5 DR. **(B)** Band gap estimation for parent Nb_2O_5 using Tauc's plot method.

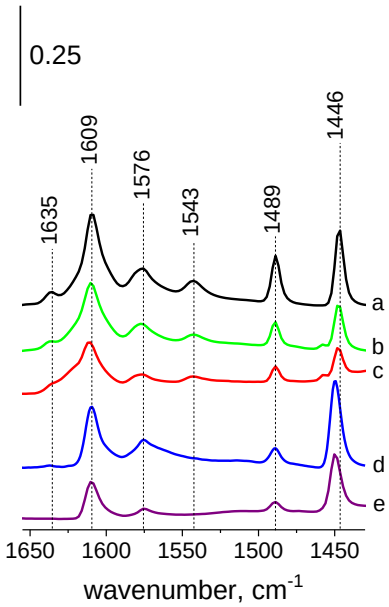

Fig. 4. FTIR spectra of (a) Nb_2O_5, (b) Au-Nb_2O_5 AP, (c) Au-Nb_2O_5 DR, (d) Cu-Nb_2O_5, (e) AuCu-Nb_2O_5 DR after Py adsorption followed by evacuation at 150 °C. The spectra were subtracted from the spectra of the activated samples before Py adsorption and normalized to mass of wafer = 13.0 mg.

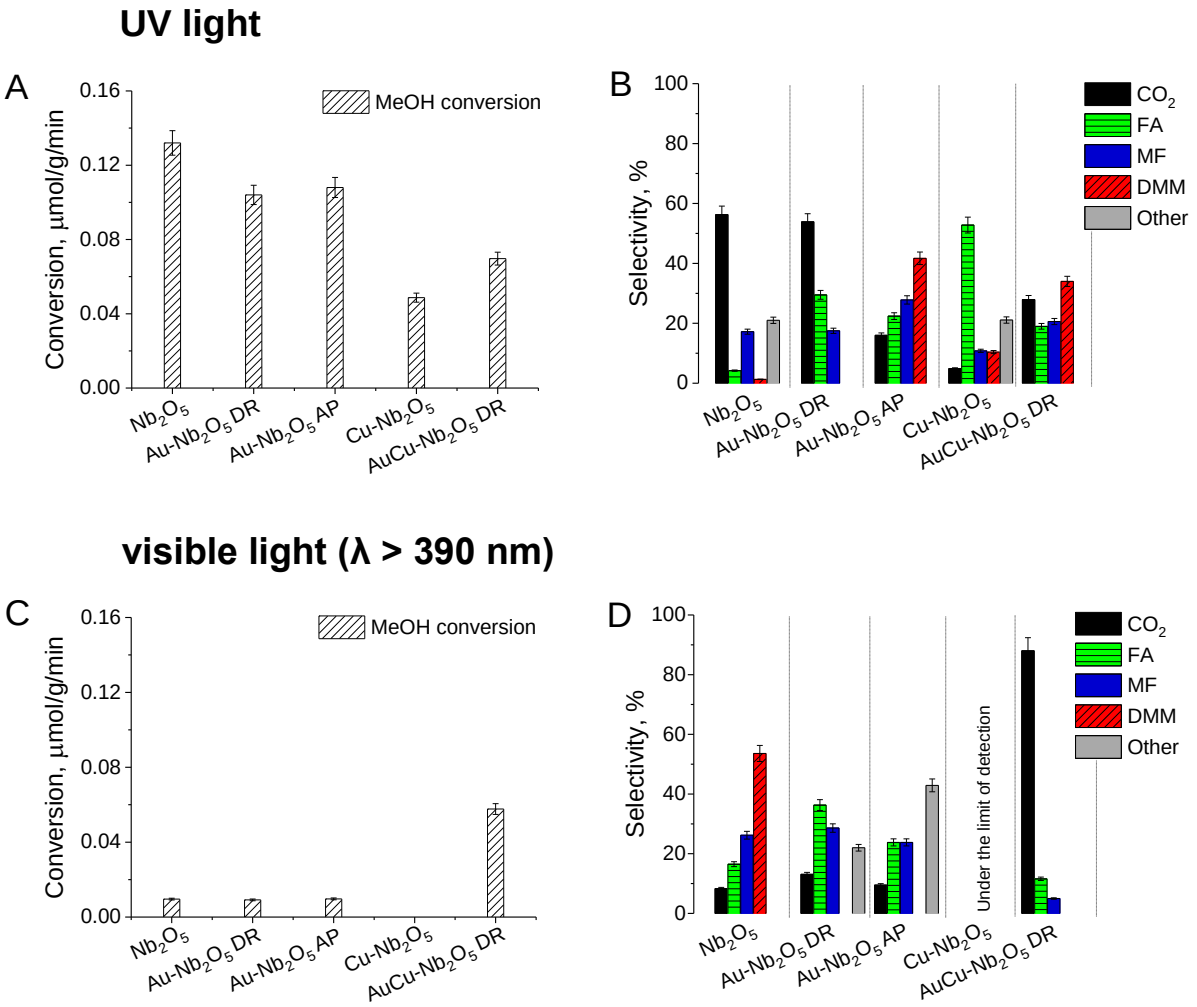

Fig. 5. Activity (**A, C**) and selectivity (**B, D**) of the catalysts at the steady state during the photocatalytic oxidation of methanol under UV irradiation (irradiance ≈ 205 mW/cm^2) and visible light irradiation (λ > 390 nm; irradiance ≈ 190 mW/cm^2).

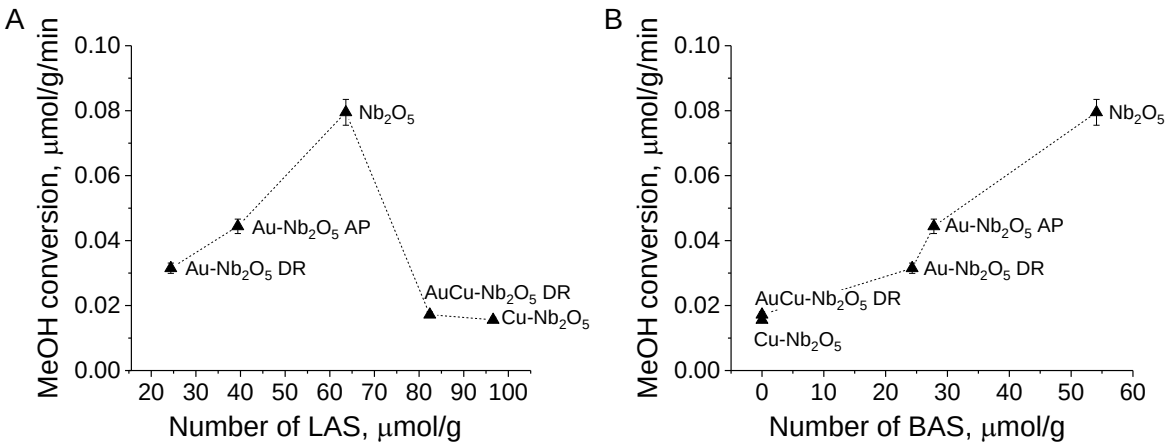

Fig. 6. The influence of Lewis **(A)** and Brønsted **(B)** acidity of the catalysts on their activity in methanol photooxidation (UV light, light intensity ≈ 70 mW/cm^2).

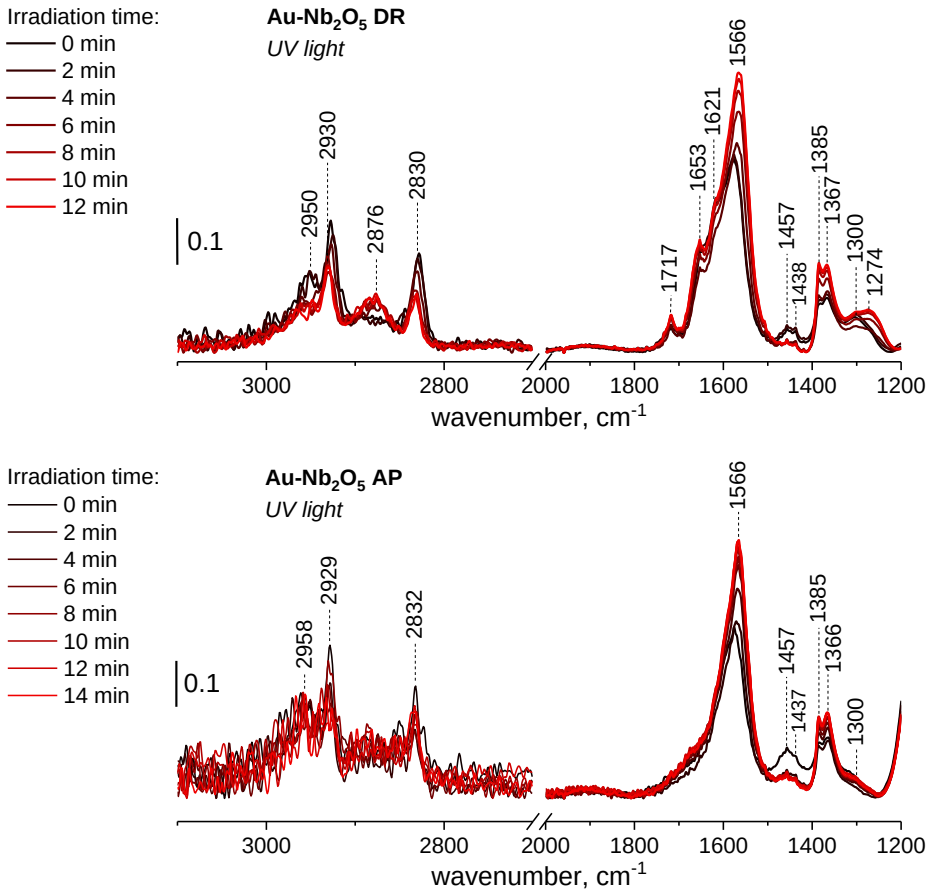

Fig. 7. IR spectra of the adsorbed surface species on Au-Nb_2O_5 DR and Au-Nb_2O_5 AP during the first minutes of irradiation with UV light (light intensity ≈ 205 mW/cm^2). The spectra were subtracted from the IR spectra of the samples before irradiation.

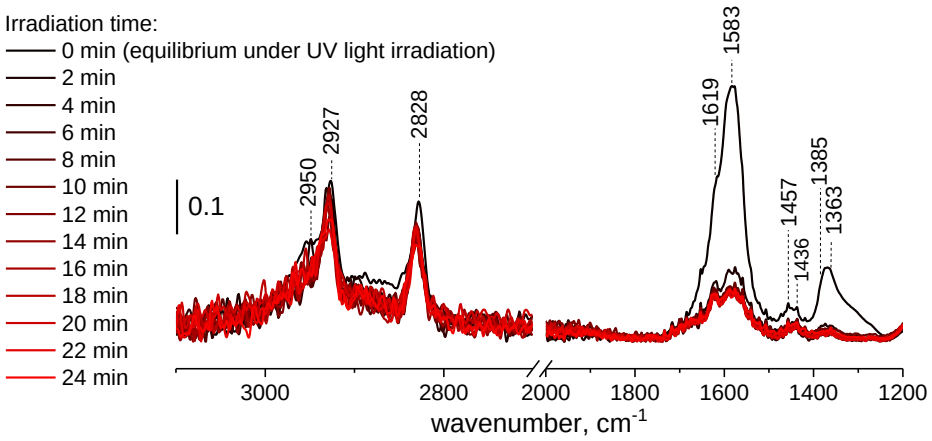

Fig. 8. IR spectra of the adsorbed surface species on AuCu-Nb_2O_5 DR during the first minutes of irradiation with visible light ($\lambda > 390$ nm; light intensity ≈ 190 mW/cm^2). The spectra were subtracted from the IR spectra of the sample before irradiation.